NANOPARTICLES-EFFECT ON THE MECHANICAL AND ELECTRICAL PROPERTIES OF PET-BASED HYBRID COMPOSITES

C. N. Barbosa[a*], P. Pereira[a], F. Gonçalves[a], J. C. Viana[a]

[a]*Institute for Polymers and Composites, Department of Polymer Engineering, University of Minho, 4800-058 Guimarães, Portugal*
**cbnuno@dep.uminho.pt*

Keywords: nanoclays, carbon nanofibers, glass fibers, injection/compression molding

Abstract
This study aims at demonstrating the effect of adding different weight percentages (in the range of [1-10] wt%) of nanoclays, NC, and carbon nanofibers, CNF, on the mechanical and electrical properties of unreinforced and 20% glass fiber, GF, reinforced poly(ethylene terephthalate), PET, obtained by compression and injection molding technologies. All composites showed a good dispersion of the nanoparticles into the PET matrices. The electrical resistivity is detrimentally affected by the injection molding process and the presence of GF. Both nanoparticles tailored differently the envisaged mechanical properties of the final composites, but an increment upon the initial modulus and reduction on the deformation capabilities was found. Hybrid composites showed an improved behavior with a small increment upon the weight.

1. Introduction

The evolution of materials science and engineering research has been offering huge advancements over the plastic industry. One of the greatest developments is related to the polymer-based composites which intend to make the "world" lighter and resilient. Polymers' raw properties can be improved by reinforcing the host matrix with e.g. glass fibers (GF) [1, 2], nanoclays (NC) [3-5], or carbon nanofibers (CNF) [6-9], among other reinforcement types. Several nanocomposite systems are deeply reviewed [10, 11] on their experimental trends (e.g. preparation, processing, and testing). More recently, a new class of materials – hybrid composites – has been studied and developed. On this research field, some authors have recently reported the possibility of tailoring the glass fiber/matrix properties by adding nanoreinforcements into the system [12-14]. In the current work, different nano and hybrid poly(ethylene terephthalate), PET-based composites were prepared/processed/tested by hosting NC or CNF into unreinforced and GF reinforced PET matrices.

NC and CNF are two groups of nanoparticles that have been widely used for the preparation of polymer nanocomposites. The value-added and multifunctionality capacities make these nanofillers very promising candidates as superior reinforcements in modern polymer industry. NC-reinforced polymers have improved, for instance, mechanical and thermal properties [3-5]; CNF-reinforced polymers are enhanced in terms of electrical and mechanical properties [6-9]. Still, technical barriers (e.g. polymer-nanoparticles adhesion, nanoparticles functionalization, dispersion, distribution, and orientation) have been restraining the massive introduction of these new materials.

The incorporation of nanofillers into polymer matrices is normally achieved by the following techniques: solvent-assisted, in-situ polymerization, or melt-blending [3-8, 12, 14]. The latter is the most widely used process for producing polymer composites due to its efficiency and environmental aspects. Many researchers have focused on high shear mixing methods, such as co-rotating twin screw extruders, and reported to be a feasible particles dispersion method for the mass production of nanocomposites [9]. Other research groups have been using injection molding process to produce thermoplastic components based on nanocomposites [8, 13].
This study draws out largely the mechanical and electrical properties of PET-based (nano and hybrid) composites. Industrial processing methods, such as extrusion, injection and compression molding, were used for the preparation/processing of those composites. The present study extends the current state-of-the-art and brings value to this fast-moving research area. Its focus lies on the understanding the effect, in terms of structure and mechanical/electrical performance, of hosting different nanoparticles into unreinforced and GF reinforced PET matrices. Furthermore, the synergetic effects of nano- and micro-reinforcements as well as the multifunctional properties of the final composites are also assessed issues.

2. Experimental protocol

2.1 Raw materials

All polymers were supplied by DSM Engineering Plastics: unreinforced PET, PET00 (ARNITE D04 300) with a density of 1340 kg/m^3; and 20% glass fiber reinforced PET, PET20 (ARNITE AV2 340) with a density of 1520 kg/m^3. The organically modified MMT Cloisite15A (hereafter labelled just as C15A) was supplied by SCP Rockwood Additives. The carbon nanofiber Pyrograf III (hereafter labelled just as CNF) was supplied by Pyrograph Products Inc.

2.2 Materials blending and processing

2.2.1 Masterbatch blending

The unreinforced PET00 and both nanoparticles – C15A and CNF – were dried in a dry air dehumidifier at 120 ºC for 6 h before compounding by melt processing to produce both C15A and CNF rich masterbatches with 10 wt% of nanoclay and 20 wt% of carbon nanofibers, respectively; these blends are from now referenced as MB_1 (PET00+C15A) and MB_2 (PET00+CNF). Both MB were processed, separately, in a co-rotating twin-screw extruder using two material feeders to improve components distribution, a barrel temperature profile from 270 ºC (at the feeder) to 265 ºC (at the die) and a screw rotation velocity of 100 rpm. At the die exit (diameter ~1.5 mm) the masterbatches were forced to pass through a recirculated cold water bath to remove the heat and solidify the strand, which was then cut to length of ca. 3 mm in the pelletizer.

2.2.2 Nano- and hybrid composites blending and processing

The MB_1 and MB_2 were added to the PET materials (PET00 and PET20) in order to obtain the desired PET-based nano- and hybrid composites. For the 'dilution' process, a protocol reported elsewhere [13] was followed in order to obtain always the exact amount of 20 wt% of GF in the composites after dilution. All materials were dried at 120ºC for 6 h. Before processing, the MB and PET materials were mechanical mixed. Compression and injection molding technologies were then used to obtain, respectively, discs and dumbbell-like axisymmetric specimens. Prior to the compression molding, the desired mixtures were

blended in a lab-scale co-rotating twin screw extruder to prepare small amounts (~100 g) of pelletized nano- and hybrid composites. In the case of injection molding, the mechanical mixed materials were directly fed in the hopper. All processed materials are described in Table 1.

Nanoparticles (wt%)	Compression molding, CM		Injection molding, IM		
	00 wt% of GF	20 wt% of GF	00 wt% of GF	20 wt% of GF	
	CNF		C15A	C15A	CNF
1.00	$Mix01CNF_{CM}$		$Mix01C15A_{IM}$	$Mix01C15AGF_{IM}$	
3.00	$Mix03CNF_{CM}$	$Mix03CNFGF_{CM}$	$Mix03C15A_{IM}$	$Mix03C15AGF_{IM}$	$Mix03CNFGF_{IM}$
4.00	$Mix04CNF_{CM}$	$Mix04CNFGF_{CM}$			$Mix04CNFGF_{IM}$
5.00			$Mix05C15A_{IM}$	$Mix05C15AGF_{IM}$	
6.00	$Mix06CNF_{CM}$	$Mix06CNFGF_{CM}$			$Mix06CNFGF_{IM}$
8.00	$Mix08CNF_{CM}$				
10.0	$Mix10CNF_{CM}$	$Mix10CNFGF_{CM}$			$Mix10CNFGF_{IM}$

Table 1. Materials coding and weight percentages (wt%) of GF and nanoparticles.

The injection molding conditions were fixed according to the material data sheet. The compression molded discs were produced under optimized pressing conditions. A total of 5 compression molded samples and 20 injection molded specimens of each material have been produced. Figures 1a and 1b show the dimensions of the specimens resulting from compression and injection molding processes, respectively. While discs were evaluated under electrical loads, the dumbbell-like axisymmetric specimens were investigated either under tensile and electrical loads. The developed morphology of both geometries has been also assessed.

Figure 1. Dimensions (in millimeters) of (a) compression molded discs and (b) injection molded tensile specimens.

2.3 Morphological characterization

2.3.1 Transmission electron microscopy, TEM

Samples were ultramicrotomed with a diamond knife of Diatome on a Leica EM UC7 microtome at room temperature to give sections with a nominal thickness of 70 nm. Bright-field images were obtained at 200 kV, with a FEI TECNAI T20 electron microscope. Low-magnification images were taken at $3.8x10^4\times$ and $8.6x10^4\times$, and high magnification images were taken at $1.25x10^5\times$ and $4.0x10^5\times$. TEM images report, qualitatively, the state of dispersion of nanoparticles and the internal structure of the molded systems.

2.3.2 Scanning electron microscopy, SEM

The fractured surfaces of the samples, broken in liquid nitrogen, were examined by scanning electron microscopy, using a Nova NanoSEM 200 (FEI). Before SEM examination, all

samples were coated under vacuum with a thin gold layer, to prevent charging effects. The particle dispersion and the particle-matrix adhesion of the cryogenic fractured surfaces (perpendicular to the melt flow direction) of the molded specimens were qualitatively studied by SEM using different magnifications ($1.5x10^4$×, $7.5x10^3$× and $2.5x10^2$×). In the case of IM bars, two different regions were studied: the grip area was chosen for the electrical properties assessment, and the parallel zone was obviously selected for the mechanical properties characterization.

2.4 Electrical characterization

The volume electrical resistivity of the nano- and hybrid composites has been evaluated at room temperature (23 ± 2 ºC) for the compression molded discs; similar characterization was carried out on the hybrid composites obtained by injection molding. Prior to the volume resistivity measurements, small samples (diameter ~8 mm) were cut from the molded specimens (as schematized in Figure 2) and then a controlled sanding operation was applied on both outer planes to guarantee the electrical measurement.

Figure 2. Schematic design of the machining operation needed to remove small disc samples (of 8 mm diameter) from (a) compression molded discs and (b) injection molded bars.

Volume electrical resistivity (Ωcm) stands for the electrical resistance through units of volume of an insulating material and can be calculated by equation (1), where ρ_v is the volume resistivity, K_v the effective area of the electrode, τ the average thickness of the sample (or distance between electrodes), and R is the bulk electrical resistance. The obtained results are the average of at least three samples from each processing method.

$$\rho_v = \frac{K_v}{\tau} R \qquad (1)$$

2.5 Mechanical characterization

The tensile properties have been evaluated on the hybrid composites obtained by hosting different amounts of two different nanoparticles in the PET20 matrix. As follows, the effect of the nanoparticles on the overall mechanical performance has been depicted. These tests were carried out at room temperature (23 ± 2 ºC) and at a cross-head velocity of 1 mm/min. The tensile tests have been performed to assess the Young's modulus (E), the stress at yield (σy), and the strain at break (εb) from the homogeneous stress-strain curves. The reported results are the average of at least six samples.

3. Results and discussion

3.1 From the morphology observations

Morphological studies were carried out as fundamental methods to understand the effects of the nanoparticles on the envisaged properties of the composites. SEM analyses of the C15A-

based composites were performed to investigate the effect of different amounts of C15A on the morphological structure of the fractured surfaces; some SEM images can be assessed elsewhere [13]. A fair interfacial adhesion between nanoclay and polymer matrix as well as minor nanoclay tactoides/agglomerates was observed. SEM investigations on CM discs (with and without GF) and IM bars (with GF) containing 3, 6 and 10 wt% of CNF are shown in Figure 3. In general, no agglomerations were found, a uniform distribution and a regular CNF dispersion in both PET matrices and geometries were achieved. Minor pulled-out of CNF from the matrix was detected. These features may indicate a need of enhancing the interfacial adhesion between the phases, which may be important to improve the mechanical performance.

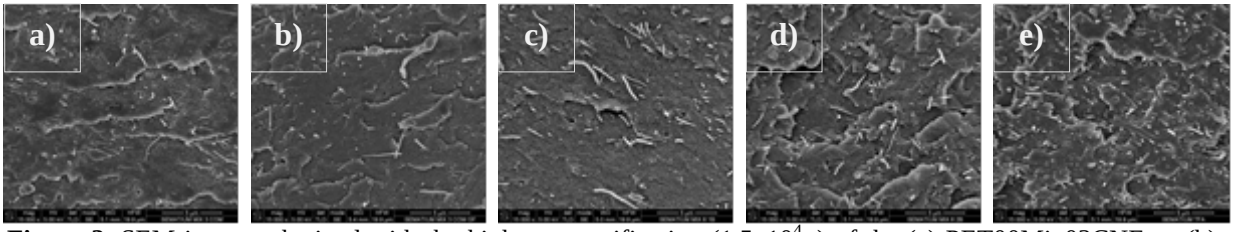

Figure 3. SEM images obtained with the highest magnification ($1.5x10^4\times$) of the (a) PET00Mix03CNF$_{CM}$, (b) PET20Mix03CNF$_{CM}$, (c) PET00Mix06CNF$_{CM}$, (d) PET20Mix06CNF$_{CM}$ and (e) PET20Mix10CNF$_{IM}$.

From TEM analyses (Figure 4), the following main observations were noticed: good CNF dispersion in the PET matrices and no significant orientation of the CNF in all composites. The close distance between CNF, some of them touching each other, may perceive a 3D network of CNF for compositions with higher weight percentages of CNF (e.g. Mix10CNFGF$_{IM}$). TEM and x-ray diffraction analyses of the C15A-based composites are revised elsewhere [13] and showed an intercalated rather than fully exfoliated structure in the MB$_1$ (Figure 4d). The injection molded samples revealed changes in the morphology of the composites with a reduced basal distance.

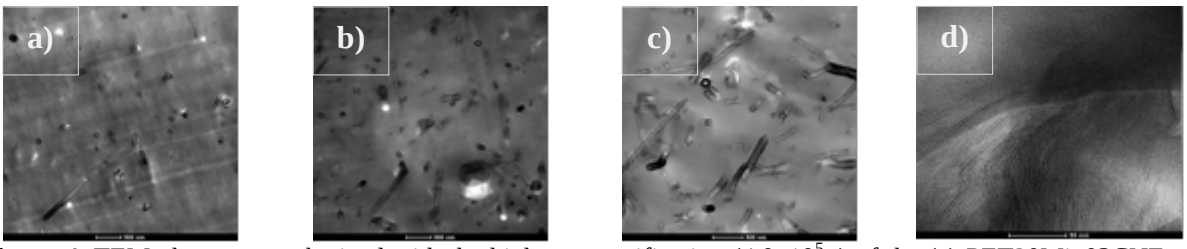

Figure 4. TEM photograms obtained with the highest magnification ($4.0x10^5\times$) of the (a) PET20Mix03CNF$_{IM}$, (b) PET20Mix06CNF$_{IM}$, (c) PET20Mix10CNF$_{IM}$ and (d) MB$_1$.

3.2 From the electrical measurements

The synergy between nano- and micro reinforcements among discs compositions obtained by compression molding as well as the effect of both molding technologies on the volume resistivity have been addressed. The purpose is to study separately the effect of multi-scale fillers and the influence of processing on the envisaged electrical property. Figure 5 evidences the results of the volume electrical resistivity measurements for the nano- and hybrid composites as a function of the weight percentage of CNF and for the two processing techniques. The relative drop of the electrical resistance, in comparison to the raw materials (PET00 and PET20), is also perceived.

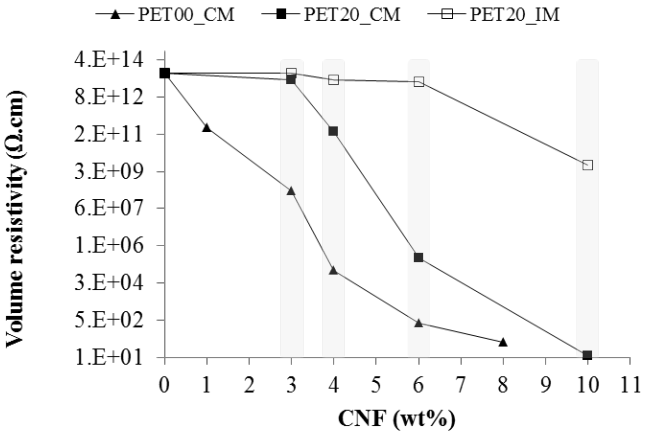

Figure 5. Volume electrical resistivity values of the nano- and hybrid CNF PET-based composites obtained by compression, CM, and injection molding, IM.

Concerning the effect of the glass fiber on the volume resistivity of the CM composites, it is clear that the presence of the GF increases the overall electrical resistivity of the material. For instance, while PET00-CM nanocomposites with 1 wt% of CNF reports a volume resistivity of ca. $2x10^{11}$ Ωcm, PET20 hybrid composites just reach this value with 4 wt% of incorporation of CNF. Moreover, the former shows a percolation threshold range for CNF loads below 3 wt% and the later presents the percolation threshold at values below 5 wt% of CNF. The presence of the GF delays the percolation threshold and, consequently, the combination of CNF and GF in the same host matrix does not enhance the electrical conductive path, at least for CM. From the SEM images (Figure 3) no major differences on the nanofiber arrangement were found between the nano- and hybrid composites meaning that the micro reinforcement (GF) is neither improving nor decrementing the state of the dispersion of CNF.

The molding process shows a strong influence on the volume electrical resistivity. PET-based hybrid composites with different weight percentages of CNF where used to compare the effect of each processing technique. The injection molding process, delays the decrement of the electrical conductivity of the composites. The volume electrical resistivity of the CM PET20 samples with 4 wt% of CNF is just comparable to the IM hybrid composites with 10 wt% of CNF. The percolation threshold of the PET-based hybrid composites obtained for IM samples is expectantly attained with CNF loads higher than 10 wt%. The thermomechanical environment imposed during the conventional injection molding process, e.g. high shear rate levels and pressures, strongly affects the final microstructure of the material systems which is, in our understanding, unfavorable to the electrical conductivity. The induced high orientation does not allow the CNF to be at enough closer distances or in contact, thus not increasing the electrical conductivity.

3.3 From the mechanical testing

The effect of each nanoparticle on the envisaged mechanical properties of the injection molded tensile specimens has been evaluated. Figure 6 presents the results of the (a) stress at yield, (b) strain at break, and (c) Young's modulus, as a function of nanoparticles content (C15A and CNF) for PET20 system. Regarding the stress at yield, it increases by adding higher amounts of CNF into the PET20 matrix; this maximum was observed for 10 wt% of CNF with an increment of 26% in comparison to the neat PET20. On the other hand, an increase on the stress at yield of the C15A hybrid composites is only observed for additions of 1 wt% of C15A (with an improvement of 14% with respect to the neat PET20). However, such small amount of C15A provides a similar effect on the stress at yield as the CNF hybrid

composite with 4 wt%. The PET20+CNF nanocomposite presents a stronger nanofiller-polymer interaction than the PET20+C15A.
By increasing the C15A content into the matrix, the strain at break decreases of about 51% in comparison to PET20. The CNF-based hybrid composites also show a drop (despite with a lower slope than the C15-based materials systems) on the elongation at break as a function of the CNF content.

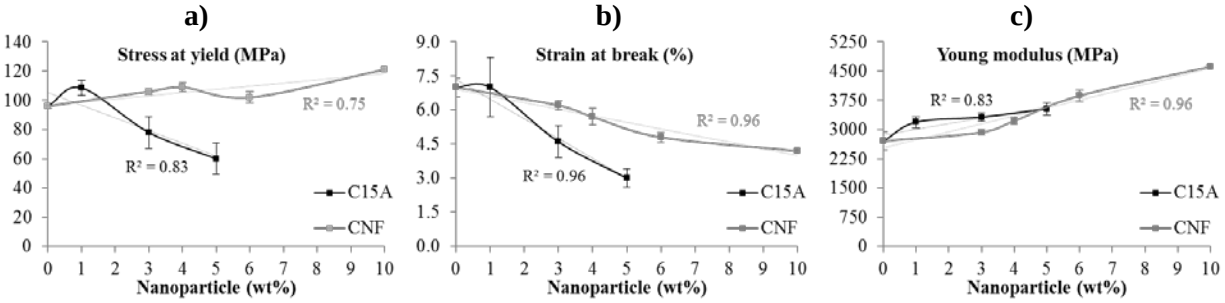

Figure 6. Main mechanical properties results of the hybrid composites obtained by injection molding.

The addition of nanoparticles into the polymer matrices induces greater stiffness on the final material. In this case, the C15-based composites are stiffer than the PET20CNF for lower nanoparticles loads. By hosting only 1 wt% of C15A into the PET20 matrix, an increase of ca. 22% on the Young's modulus is achieved which is just possible with CNF on the range of 4 < wt% < 6. The hybrid composite with 10 wt% of CNF presents the highest stiffness with a variation of +77% in comparison to the neat PET20. *E* appears to increase almost linearly with the increment upon the filling of the nanoparticles, regardless of their type.

4. Conclusions

The morphological state of the studied materials, assessed by TEM and SEM, revealed in the case of C15A-based composites the existence of a nanoclay intercalated structure in the MB_1; the subsequent injection molding process changed the morphology of the composites reducing the basal distance. Regarding the CNF-based composites, a good dispersion of the nanofibers was achieved without clusters.
The incorporation of CNF induces a decrease upon the electrical resistivity. Although, the observations revealed this property is affected by the presence of the glass fibers in the hostage matrix that reduces this variation. Also, it was verified that the processing methodology strongly influences the electrical resistivity, which is significantly decreased (ca. 6 orders of magnitude) for compression molded samples when compared to the injection moldings. The latter processing technique markedly delays the percolation limit.
Generally, both C15A and CNF upgraded the mechanical properties of the final compositions. The initial modulus increases almost linearly with the incorporation of the nanoparticles, reaching an increment of 77% for 10 wt% of CNF. The used nanoparticles impart different variations upon the yield stress. The yield stress of C15A hybrid PET composite shows a maximum for low percentage of incorporation (1 wt%), but then decreases largely thereafter. However, for the case on CNF filled hybrid PET composite the yield stress increases with the amount of CNF added. For both cases, the strain at break decreases with the incorporation of the nanoparticles (except for 1 wt% of C15A), with higher decrement (51%) for the nanoclay filled hybrid PET composite. In the case of C15A-based composites, all envisaged mechanical properties were simultaneously enhanced by adding 1 wt% of C15A into the PET20 matrix.

References

[1] I. Rezaeian, S. Jafari, P. Zahedi, and S. Nouri. An investigation on the rheology, morphology, thermal and mechanical properties of recycled poly(ethylene terephthalate) Reinforced With Modified Short Glass Fibers. *Polymer Composites*, volume (30): 994-999, 2009.

[2] M. Krácalík, L. Pospísil, M. Slouf, J. Mikesová, A. Sikora, J. Simoník, and I. Fortelný. Effect of glass fibers on rheology thermal and mechanical properties of recycled PET. *Polymer Composites*, volume (29), 915-921, 2008.

[3] R. Rajeev, E. Harkin-Jones, K. Soon, T. McNally, G. Menary, C. Armstrong, and P. Martin. Studies on the effect of equi-biaxial stretching on the exfoliation of nanoclays in polyethylene terephthalate. *European Polymer Journal*, volume (45), 332-340, 2009.

[4] C. Calcagno, C. Mariani, S. Teixeira, and R. Mauler. The effect of organic modifier of the clay on morphology and crystallization properties of PET nanocomposites. *Polymer*, volume (48), 966-974, 2007.

[5] J. Bandyopadhyay, S. Ray, and M Bousmina. Thermal and thermo-mechanical properties of poly(ethylene terephthalate) nanocomposite. *Journal of Industrial and Engineering Chemistry*, volume (13), 614-623, 2007.

[6] H. Ma, J. Zeng, M. Realff, S. Kumar, and D. Schiraldi. Processing, structure, and properties of fibers from polyester/carbon nanofiber composites. *Composites Science and Technology*, volume (3), 1617-1628, 2003.

[7] G. Sui, S. Jana, W-H Zhong, M. Fuqua, and C. Ulven. Dielectric properties and conductivity of carbon nanofibers/semi-crystalline polymer composites. *Acta Materialia*, volume (56), 2381-2388, 2008.

[8] M. Al-Saleha, and U. Sundararaj. Electrically conductive carbon nanofibers/polyethylene composite: Effect of melt mixing conditions. *Polymers for Advanced Technologies*, volume (22), 246-253, 2011.

[9] K. Enomoto, T. Yasuhara, and N. Ohtake. Mechanical properties of injection-molded composites of carbon nanofibers in polypropylene matrix. *New Diamond and Frontier Carbon Technology*, volume (15), 59-72, 2005.

[10] S. Ray, and M. Okamoto. Polymer/layered silicate nanocomposite: Review from preparation to processing. *Progress in Polymer Science*, volume (28), 1539–1641, 2003.

[11] G. Tibbetts, M Lake, K. Strong, and B. Rice. A review of the fabrication and properties of vapor-grown carbon nanofibers/polymer composites. *Composites Science and Technology*, volume (67), 1709-1718, 2007.

[12] T. Wan, S. Liao, K. Wang, P. Yan, and M. Clifford. Multi-scale hybrid polyamide 6 composites reinforced with nano-scale clay and micro-scale short glass fibre. *Composites: Part A*, volume (50), 31-38, 2013.

[13] C. Barbosa, F. Gonçalves, and J. Viana. Nano and hybrid composites based on poly(ethyleneterephthalate): Blending and characterization. *Advances in Polymer Technology*, volume (33), DOI: 10.1002/adv.21397, 2014.

[14] N. Isitman, H. Gunduz, and C. Kaynak. Nanoclay synergy in flame retarded/glass fibre reinforced polyamide 6. *Polymer Degradation and Stability*, volume (94), 2241-2250, 2009.